Diamond p-Type Lateral Schottky Barrier Diodes With High Breakdown Voltage (4612 V at 0.01 mA/Mm)

Zhuoran Han and Can Bayram, *Senior Member, IEEE*

***Abstract*— Diamond p-type lateral Schottky barrier diodes (SBDs) with a 2-μm-thick drift layer are fabricated with and without Al_2O_3 field plates. Schottky contacts composed of Mo (50 nm) / Pt (50 nm) / Au (100 nm) showed a barrier height of 1.02 $\pm$ 0.01 eV and ohmic contacts of Ti (30 nm) / Pt (30 nm) / Au (100 nm) achieved a specific ohmic contact resistance of 1.25 $\pm$ 0.98 x 10^{-4} Ω-cm^2. Their forward and reverse bias characteristics are studied in detail. Both SBDs, with and without Al_2O_3 field plates, exhibit rectifying ratios larger than 10^7 at room temperature, and a peak current density of 5.39 mA/mm under 40 V forward bias at 200 °C. The leakage current density at room temperature is stable at approximately 0.01 mA/mm for both diodes. The SBD without the Al_2O_3 field plate exhibited a breakdown voltage of 1159 V, while the SBD with the Al_2O_3 field plate is stable under a reverse voltage of 4612 V, which is higher than many diamond SBDs previously reported.**

***Index Terms*— Diamond, Schottky barrier diode, breakdown voltage, Al_2O_3.**

I. Introduction

DIAMOND is an emerging semiconductor for high-power electronics with its large bandgap (E_G, 5.47 eV), large critical E-field (E_B, 10 – 20 MV/cm), high carrier mobility (μ, up to 2100 cm^2$\cdot$ V^{-1}$\cdot$ s^{-1} for holes at low doping concentrations ($< 10^{15}$ cm^{-3})), and high thermal conductivity (k, 22 - 24 W$\cdot$ cm^{-1}$\cdot$ K^{-1}) [1]. The relatively low activation energy of p-type boron dopants (0.38 eV compared to 0.57 eV for n-type phosphorus) and the maturation of CVD grown boron-doped diamond motivate p-type diamond Schottky diodes for studies [2] and high critical fields of 7.7 MV/cm [3] and breakdown voltages of 2.5 kV [4] have been demonstrated in either vertical or pseudo-vertical configurations. Increasing the breakdown voltages higher in these devices require increasing the drift layer thickness [5], which is challenging to grow experimentally [6], [7], as well as etching deeper, which creates processing issues [8]. One way to scale diamond SBD to higher voltage is using their lateral configuration, where breakdown voltages are scaled via adjusting the distance between the anode and cathode, without the need for a thick drift layer.

In this letter, diamond p-type lateral Schottky barrier diodes (SBDs) with high breakdown voltage (4612 V) enabled with contact regrowth and edge termination techniques are reported. Forward I-V characteristics are studied using the thermionic emission model and the Mott-Gurney relation. The SBDs are simulated under reverse bias using Synopsys' Sentaurus TCAD software to investigate the effect of the field plate structures. The simulation predicts a significant reduction in the peak electric field with the addition of the field plate, which agrees with the breakdown performance of diodes with and without the field plate measured by experiments. Finally, the lateral SBDs are benchmarked against previously reported diamond power devices in terms of specific on-resistance (R_{ON}) and breakdown voltage (V_{br}).

II. Device Fabrication

Fig. 1 shows the epitaxy (by microwave plasma enhanced chemical vapor deposition (MPCVD)) and cleanroom microfabrication process flow of diamond p-type lateral SBDs. First, a 2 μm p$^-$drift layer ([B] $< 8 \times 10^{15}$ cm^{-3}]) was grown on a 3 $\times$ 3 mm^2 Type Ib (100) high pressure high temperature (HPHT) diamond substrate. The RMS surface roughness of the epitaxial layer was measured to be 7.5 nm using optical profilometry. Then, 200 nm p$^+$diamond ([B] $\sim$ 3×10^{20} cm^{-3}]) was selectively grown to form the ohmic contact region. Ohmic metal contacts were formed by e-beam evaporation of Ti (30 nm) / Pt (30 nm) / Au (100 nm), followed by thermal annealing at 450 °C in an ambient of Ar gas for 50 minutes. The specific contact resistance of ohmic contacts was determined by TLM measurements and measured to be 1.25 $\pm$ 0.98 $\times$ 10^{-4} Ω-cm^2. Next, a 300 nm Al_2O_3 field plate was deposited by e-beam evaporation, followed by a lift-off process. Al_2O_3 was chosen as the field oxide because of its high dielectric constant relative to diamond (k=8.63 $\pm$ 0.07 for the as-deposited Al_2O_3) that reduces the electric field strength and a large band offset for the oxygen-terminated diamond [9], [10]. The exposed diamond surface was ozone treated at room temperature for 1.5 hours to obtain a stable oxygen termination prior to the Schottky contact deposition [11]. Schottky metal stack of Mo (50 nm) / Pt (50 nm) / Au (100 nm) was deposited by e-beam

Manuscript received 12 June 2023; revised 15 August 2023; accepted 29 August 2023. Date of publication 31 August 2023; date of current version 27 September 2023. The review of this letter was arranged by Editor S. Chowdhury. *(Corresponding author: Can Bayram.)*

The authors are with the Department of Electrical and Computer Engineering, University of Illinois at Urbana–Champaign, Champaign, IL 61820 USA (e-mail: cbayram@illinois.edu).

Color versions of one or more figures in this letter are available at https://doi.org/10.1109/LED.2023.3310910.

Digital Object Identifier 10.1109/LED.2023.3310910

This work is licensed under a Creative Commons Attribution-NonCommercial-NoDerivatives 4.0 License.
For more information, see https://creativecommons.org/licenses/by-nc-nd/4.0/

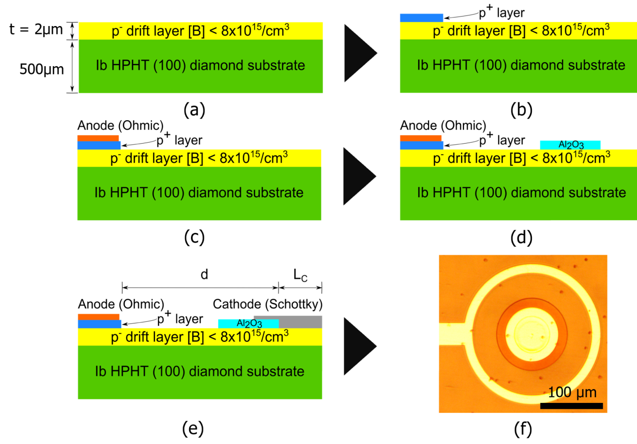

Fig. 1. Epitaxy and cleanroom microfabrication steps for diamond lateral SBDs (a) p^- drift layer epitaxial growth; (b) p^+ contact layer selective growth; (c) ohmic contacts deposition; (d) Al_2O_3 field plates formation; (e) Schottky contacts deposition; (f) top view microscope image of a fabricated diamond lateral SBD with the field plate.

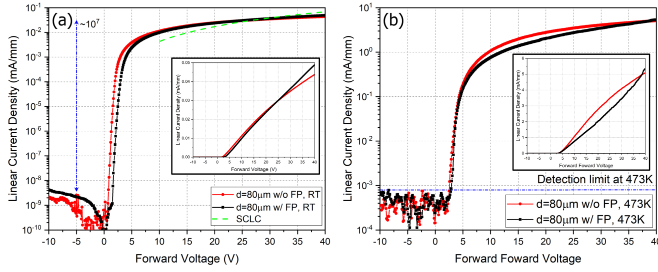

Fig. 2. (a) Forward J-V characteristics of diamond lateral SBD with and without the field plate (FP) in semi-logarithmic and (inset) linear scales at room temperature (RT); the dashed line represents the calculated space charge limited conduction (SCLC) J-V relation. (b) Forward J-V characteristics of diamond lateral SBD with and without the FP in semi-logarithmic and (inset) linear scales at 200 °C.

evaporation. The inner and outer radii of the Al_2O_3 field plate are 40 μm and 80 μm, respectively. The radius of the Schottky contact is 60 μm, and the separation between the ohmic and Schottky contact is $d = 80$ μm. The top-view microscope image of the fabricated circular structure diamond p-type lateral SBD with the field plate is shown in Fig. 1(f).

III. Results and Discussion

Fig. 2(a) shows the semi-logarithmic and linear (inset) J-V curves of fabricated diamond p-type lateral SBD with and without the Al_2O_3 field plate at room temperature. The SBD without the field plate has the same Schottky to ohmic distance $d = 80$ μm, and the Schottky contact radius is the same as the inner radius of the Al_2O_3 field plate. Both diodes exhibit a rectifying ratio of 10^7 in the range of +/− 5 V. The linear current densities at a 40 V forward bias are 0.049 mA/mm and 0.044 mA/mm for the SBD with and without the field plate, respectively. The SBDs were reprocessed several times before high-temperature and breakdown measurements and showed good reproducibility in forward J-V characteristics. The max difference in forward current densities at the 40 V forward bias between four fabrication batches is 15% and 6% for the SBD with and without the FP, respectively. The Schottky barrier

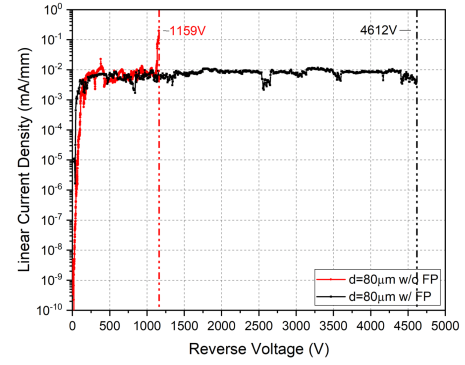

Fig. 3. Room temperature reverse leakage J-V characteristics of diamond lateral SBD with and without the FP.

height (SBH) at zero bias are estimated using the thermionic emission model from the fitting of the log-linear regions of the forward J-V curve:

$$J_S = A^* T^2 \exp(\frac{-q\phi_B}{k_B T}) \quad (1)$$

$$J = J_S \times \left[\exp\left(\frac{qV}{nk_B T}\right) - 1\right] \quad (2)$$

where J_S, A^*, T, n, q, ϕ_B, and k_B are reverse saturation current density, Richardson constant (90 A cm^{-2} K^2 for diamond [12]), absolute temperature, ideality factor, elementary charge, SBH, and Boltzmann constant, respectively. The extracted ideality factor for SBD with and without the field plate is 4.77 and 3.71, respectively. The SBH estimated from the fittings of four fabricated SBDs is 1.02 ± 0.01 eV. The SBH is in close agreement to other Mo-diamond Schottky contacts in lateral devices previously reported [13].

Fig. 2(a) also plots the calculated space charge limited conduction (SCLC) current density for 10 – 40V forward voltages in the fabricated diodes. Due to dopants incomplete ionization at room temperature, the active hole concentration in the drift region is estimated to be lower than 10^{14} cm^{-3}. As the applied forward bias increases, charge neutrality is no longer maintained as injected charges accumulate in the drift region, and the SCLC begins to dominate [14]. For a lightly doped semiconductor, the SCLC is described by the Mott-Gurney relation:

$$J = \frac{9}{8}\epsilon_r \epsilon_0 \mu \frac{V^2}{d^3} \quad (3)$$

where J, ϵ_r, ϵ_0, μ, V, and d are current density, relative dielectric permittivity, permittivity of free space, carrier mobility, voltage across the drift region and length of the drift region, respectively. The calculated SCLC current is in close agreement with the measured data. At 200 °C, most acceptors become ionized and the linear current density at a 40 V forward bias increased significantly to 5.39 mA/mm and 5.09 mA/mm for SBD with and without the field plate respectively as shown in Fig. 2(b).

Fig. 3 shows the reverse leakage J-V characteristics of the SBD with and without the field plate. The diamond wafer was submerged in 3M™Fluorinert™electronic liquids during reverse measurement to prevent air breakdown. The

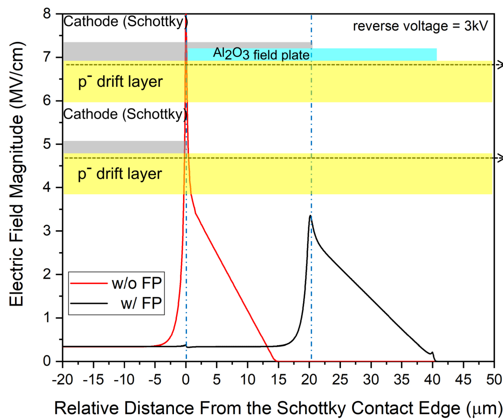

Fig. 4. Simulated horizontal electric field magnitude along the dashed cutlines at 0.1 μm away from the diamond-Schottky contact interface for lateral SBD with and without FPs at a reverse bias voltage of 3 kV.

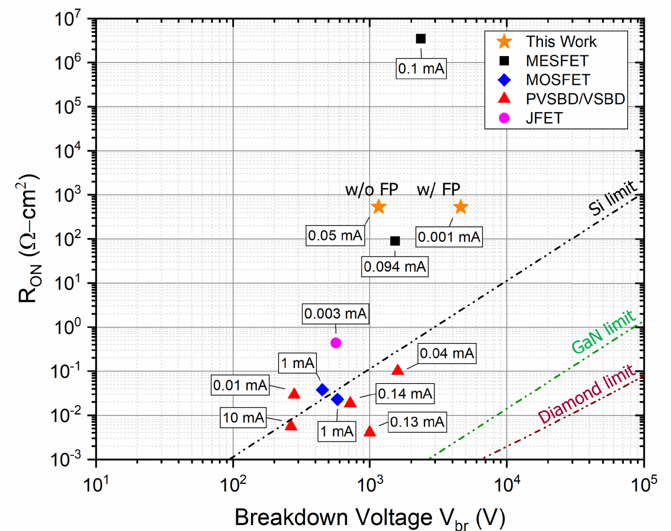

Fig. 5. Benchmark of the fabricated lateral SBDs compared with previously reported diamond power devices including lateral MESFETs, MOSFETs and junction FETs, and pseudo-vertical and vertical SBDs at room temperature. The leakage currents at which the breakdown is reported are shown in the brackets.

lateral SBD without the field plate broke down at 1159 V, when leakage current drastically increased to the compliance limit of 50 μA. After the first breakdown, reverse current density increased at low reverse bias, which confirmed the generation of leakage paths. No physical damage to the Schottky contact was identified post measurement. However, repeated breakdown measurements showed a decrease in the breakdown voltage. The SBD with the field plate exhibited stable leakage current up to 4612 V, which is the limit of the Fluorinert™electronic liquids. The leakage current density at 4612 V reverse bias is less than 0.01 mA/mm, which is similar to that of the SBD without the field plate prior to breakdown. The relatively high stable leakage current can be attributed to high surface roughness of the epitaxially grown drift layer (RMS roughness = 7.5 nm), caused by rough polishing and random growth defects.

Fig. 4 shows the simulated horizontal electric field magnitude along the dashed cutlines at 0.1 μm away from the diamond-Schottky contact interface for lateral SBD with and without the field plate at a reverse bias voltage of 3 kV. Synopsys Sentaurus TCAD software is used to study the effect of the Al_2O_3 field plate. An empirical mobility model [15], impact ionization coefficients for the model of Overstraeten and Man [16], incomplete ionizations of dopants and Schottky barrier lowering due to image forces are incorporated. Electric field magnitude is examined across the drift region near the metal-semiconductor interface where the electric field crowding is severe. The simulation predicts a 56% reduction in peak electric field near the edge of the Schottky contact with the addition of the 300 nm thick Al_2O_3 field plate.

Fig. 5 shows a benchmark of specific on-resistance (R_{ON}) vs. breakdown voltage (V_{br}) [13], [17], [3], [18], [19], [20], [21], [22], [23] at room temperature. This work exhibits a higher breakdown voltage than previously reported pseudo-vertical and vertical SBDs, lateral MESFETs, MOSFETs, and JEFTs.

The specific on-resistances are normalized to be 527 Ω-cm^2 and 534 Ω-cm^2 for SBD with and without the field plate, respectively. The R_{ON} values are 3 to 4 orders of magnitude higher than state-of-the-art pseudo-vertical and vertical SBDs. Given the low specific contact resistance ($1.25 \pm 0.98 \times 10^{-4}$ Ω-cm^2) of the ohmic contact, the large R_{ON} can be attributed to the space charge limited conduction (SCLC) and the space charge region in p^- drift layer associated to the n-type type Ib diamond substrate which reduces the active layer thickness for current conduction. R_{ON} can be optimized through a study of the drift layer thickness and doping. A thicker channel can increase the linear current density [20], thus lowering R_{ON}. The drift layer doping concentration can also be increased to overcome SCLC and allow for a shorter drift layer.

IV. Conclusion

In conclusion, diamond p-type lateral SBDs with and without the Al_2O_3 field plate are reported. At room temperature, the diodes exhibit a rectifying ratio of 10^7 and have forward current densities of 0.049 (with field plate) and 0.044 (without field plate) mA/mm at 40 V forward bias. The specific on-resistances are 534 (without field plate) and 527 (with field plate) Ω-cm^2. Under reverse bias, both diodes show leakage current densities lower than 0.01 mA/mm prior to breakdown. The Al_2O_3 field plate increases the breakdown voltage from 1159 V to 4612 V, with no discernable effects on the I-V behavior. The effect of the Al_2O_3 field plate is studied with TCAD simulation using Synopsys' Sentaurus software, which predicted a 56% reduction in peak electric field magnitude using the Al_2O_3 field plate at a reverse bias voltage of 3 kV. Finally, a benchmark of the lateral SBDs in terms of specific on-resistance vs. breakdown voltage is presented. The breakdown voltage is one of the highest so far among p-type diamond Schottky diodes. However, further optimizations of the drift layer thickness and doping concentration are needed to reduce R_{ON} and get closer to the material limit of diamond.

REFERENCES

[1] N. Donato, N. Rouger, J. Pernot, G. Longobardi, and F. Udrea, "Diamond power devices: State of the art, modelling, figures of merit and future perspective," *J. Phys. D, Appl. Phys.*, vol. 53, no. 9, Feb. 2020, Art. no. 093001, doi: 10.1088/1361-6463/ab4eab.

[2] J.-P. Lagrange, A. Deneuville, and E. Gheeraert, "Activation energy in low compensated homoepitaxial boron-doped diamond films," *Diamond Rel. Mater.*, vol. 7, no. 9, pp. 1390–1393, Sep. 1998, doi: 10.1016/S0925-9635(98)00225-8.

[3] A. Traoré, P. Muret, A. Fiori, D. Eon, E. Gheeraert, and J. Pernot, "Zr/oxidized diamond interface for high power Schottky diodes," *Appl. Phys. Lett.*, vol. 104, no. 5, Feb. 2014, Art. no. 052105, doi: 10.1063/1.4864060.

[4] D. J. Twitchen, A. J. Whitehead, S. E. Coe, J. Isberg, J. Hammersberg, T. Wikstrom, and E. Johansson, "High-voltage single-crystal diamond diodes," *IEEE Trans. Electron Devices*, vol. 51, no. 5, pp. 826–828, May 2004, doi: 10.1109/TED.2004.826867.

[5] G. Chicot, D. Eon, and N. Rouger, "Optimal drift region for diamond power devices," *Diamond Rel. Mater.*, vol. 69, pp. 68–73, Oct. 2016, doi: 10.1016/j.diamond.2016.07.006.

[6] Y. Kato, T. Teraji, T. Matsumoto, N. Tokuda, and H. Umezawa, "Key technologies for device fabrications and materials characterizations," in *Power Electronics Device Applications of Diamond Semiconductors*. Amsterdam, The Netherlands: Elsevier, 2018, pp. 219–294, doi: 10.1016/B978-0-08-102183-5.00004-2.

[7] J. Achard, F. Silva, R. Issaoui, O. Brinza, A. Tallaire, H. Schneider, K. Isoird, H. Ding, S. Koné, M. A. Pinault, F. Jomard, and A. Gicquel, "Thick boron doped diamond single crystals for high power electronics," *Diamond Rel. Mater.*, vol. 20, no. 2, pp. 145–152, Feb. 2011, doi: 10.1016/j.diamond.2010.11.014.

[8] A. Toros, M. Kiss, T. Graziosi, S. Mi, R. Berrazouane, M. Naamoun, J. V. Plestina, P. Gallo, and N. Quack, "Reactive ion etching of single crystal diamond by inductively coupled plasma: State of the art and catalog of recipes," *Diamond Rel. Mater.*, vol. 108, Oct. 2020, Art. no. 107839, doi: 10.1016/j.diamond.2020.107839.

[9] K. Ikeda, H. Umezawa, and S. Shikata, "Edge termination techniques for p-type diamond Schottky barrier diodes," *Diamond Rel. Mater.*, vol. 17, nos. 4–5, pp. 809–812, Apr. 2008, doi: 10.1016/j.diamond.2007.12.066.

[10] P. W. Peacock and J. Robertson, "Band offsets and Schottky barrier heights of high dielectric constant oxides," *J. Appl. Phys.*, vol. 92, no. 8, pp. 4712–4721, Oct. 2002, doi: 10.1063/1.1506388.

[11] T. Sakai, K.-S. Song, H. Kanazawa, Y. Nakamura, H. Umezawa, M. Tachiki, and H. Kawarada, "Ozone-treated channel diamond field-effect transistors," *Diamond Rel. Mater.*, vol. 12, pp. 1971–1975, Oct./Nov. 2003, doi: 10.1016/S0925-9635(03)00277-2.

[12] H. Umezawa, T. Saito, N. Tokuda, M. Ogura, S.-G. Ri, H. Yoshikawa, and S.-I. Shikata, "Leakage current analysis of diamond Schottky barrier diode," *Appl. Phys. Lett.*, vol. 90, no. 7, Feb. 2007, Art. no. 073506, doi: 10.1063/1.2643374.

[13] U. Choi, T. Kwak, S. Han, S.-W. Kim, and O. Nam, "High breakdown voltage of boron-doped diamond metal semiconductor field effect transistor grown on freestanding heteroepitaxial diamond substrate," *Diamond Rel. Mater.*, vol. 121, Jan. 2022, Art. no. 108782, doi: 10.1016/j.diamond.2021.108782.

[14] H. Surdi, T. Thornton, R. J. Nemanich, and S. M. Goodnick, "Space charge limited corrections to the power figure of merit for diamond," *Appl. Phys. Lett.*, vol. 120, no. 22, May 2022, Art. no. 223503, doi: 10.1063/5.0087059.

[15] A. Maréchal, N. Rouger, J.-C. Crébier, J. Pernot, S. Koizumi, T. Teraji, and E. Gheeraert, "Model implementation towards the prediction of J(V) characteristics in diamond bipolar device simulations," *Diamond Rel. Mater.*, vol. 43, pp. 34–42, Mar. 2014, doi: 10.1016/j.diamond.2014.01.009.

[16] A. Hiraiwa and H. Kawarada, "Blocking characteristics of diamond junctions with a punch-through design," *J. Appl. Phys.*, vol. 117, no. 12, Mar. 2015, Art. no. 124503, doi: 10.1063/1.4916240.

[17] J. Tsunoda, N. Niikura, K. Ota, A. Morishita, A. Hiraiwa, and H. Kawarada, "580 V breakdown voltage in vertical diamond trench MOSFETs with a P^{-}-drift layer," *IEEE Electron Device Lett.*, vol. 43, no. 1, pp. 88–91, Jan. 2022, doi: 10.1109/LED.2021.3131038.

[18] R. Kumaresan, H. Umezawa, N. Tatsumi, K. Ikeda, and S. Shikata, "Device processing, fabrication and analysis of diamond pseudo-vertical Schottky barrier diodes with low leak current and high blocking voltage," *Diamond Rel. Mater.*, vol. 18, nos. 2–3, pp. 299–302, Feb. 2009, doi: 10.1016/j.diamond.2008.10.055.

[19] J. Wang, G. Shao, Q. Li, G. Chen, X. Yan, Z. Song, Y. Wang, R. Wang, W. Wang, S. Fan, and H.-X. Wang, "Vertical diamond trench MOS barrier Schottky diodes with high breakdown voltage," *IEEE Trans. Electron Devices*, vol. 69, no. 11, pp. 6231–6235, Nov. 2022, doi: 10.1109/TED.2022.3206178.

[20] H. Umezawa, T. Matsumoto, and S.-I. Shikata, "Diamond metal–semiconductor field-effect transistor with breakdown voltage over 1.5 kV," *IEEE Electron Device Lett.*, vol. 35, no. 11, pp. 1112–1114, Nov. 2014, doi: 10.1109/LED.2014.2356191.

[21] T. Iwasaki, J. Yaita, H. Kato, T. Makino, M. Ogura, D. Takeuchi, H. Okushi, S. Yamasaki, and M. Hatano, "600 V diamond junction field-effect transistors operated at 200 °C," *IEEE Electron Device Lett.*, vol. 35, no. 2, pp. 241–243, Feb. 2014, doi: 10.1109/LED.2013.2294969.

[22] H. Umezawa, S.-I. Shikata, and T. Funaki, "Diamond Schottky barrier diode for high-temperature, high-power, and fast switching applications," *Jpn. J. Appl. Phys.*, vol. 53, no. 5S1, May 2014, Art. no. 05FP06, doi: 10.7567/JJAP.53.05FP06.

[23] K. Ikeda, H. Umezawa, N. Tatsumi, K. Ramanujam, and S.-I. Shikata, "Fabrication of a field plate structure for diamond Schottky barrier diodes," *Diamond Rel. Mater.*, vol. 18, nos. 2–3, pp. 292–295, Feb. 2009, doi: 10.1016/j.diamond.2008.10.021.